Tissue Eng Regen Med (2018) 15(6):721–733
https://doi.org/10.1007/s13770-018-0145-7

Online ISSN 2212-5469
Print ISSN 1738-2696

ORIGINAL ARTICLE

Keratinocyte Migration in a Three-Dimensional *In Vitro* Wound Healing Model Co-Cultured with Fibroblasts

Kritika Iyer[1] · Zhuo Chen[1] · Teja Ganapa[1] · Benjamin M. Wu[1,2] · Bill Tawil[1] · Chase S. Linsley[1]

Received: 4 April 2018 / Revised: 9 July 2018 / Accepted: 12 July 2018 / Published online: 14 August 2018

Abstract

BACKGROUND: Because three-dimensional (3D) models more closely mimic native tissues, one of the goals of 3D *in vitro* tissue models is to aid in the development and toxicity screening of new drug therapies. In this study, a 3D skin wound healing model comprising of a collagen type I construct with fibrin-filled defects was developed.

METHODS: Optical imaging was used to measure keratinocyte migration in the presence of fibroblasts over 7 days onto the fibrin-filled defects. Additionally, cell viability and growth of fibroblasts and keratinocytes was measured using the alamarBlue® assay and changes in the mechanical stiffness of the 3D construct was monitored using compressive indentation testing.

RESULTS: Keratinocyte migration rate was significantly increased in the presence of fibroblasts with the cells reaching the center of the defect as early as day 3 in the co-culture constructs compared to day 7 for the control keratinocyte monoculture constructs. Additionally, constructs with the greatest rate of keratinocyte migration had reduced cell growth. When fibroblasts were cultured alone in the wound healing construct, there was a 1.3 to 3.4-fold increase in cell growth and a 1.2 to 1.4-fold increase in cell growth for keratinocyte monocultures. However, co-culture constructs exhibited no significant growth over 7 days. Finally, mechanical testing showed that fibroblasts and keratinocytes had varying effects on matrix stiffness with fibroblasts degrading the constructs while keratinocytes increased the construct's stiffness.

CONCLUSION: This 3D *in vitro* wound healing model is a step towards developing a mimetic construct that recapitulates the complex microenvironment of healing wounds and could aid in the early studies of novel therapeutics that promote migration and proliferation of epithelial cells.

Keywords Collagen · Fibrin · *In vitro* model · Cell migration · Cell proliferation

1 Introduction

In healthy individuals, minor wounds readily heal and require no intervention, but larger wounds or wounds in patients with compromised immunity or poor circulation can become non-healing, progressive and chronic [1]. These chronic wounds affect nearly 6.5 million patients in the United States and costs US$25 billion annually, and these numbers are expected to rise as the population ages, more people are diagnosed with diabetes and the obesity rates increase [2]. The current standard of care includes debridement combined with infection control, off-loading

Electronic supplementary material The online version of this article (https://doi.org/10.1007/s13770-018-0145-7) contains supplementary material, which is available to authorized users.

✉ Chase S. Linsley
clinsle@ucla.edu

[1] Department of Bioengineering, University of California, Los Angeles, 420 Westwood Plaza, Room 5121, Engineering V, P.O. Box 951600, Los Angeles, CA 90095-1600, USA

[2] Division of Advanced Prosthodontics and the Weintraub Center for Reconstructive Biotechnology, School of Dentistry, University of California, Los Angeles, 10833 Le Conte Ave, Los Angeles, CA 90095, USA

to relieve pressure, and maintenance of a moist wound bed [3].

For hard-to-heal wounds, several alternative therapies for treating these chronic wounds have been developed, including acellular dermal matrices and bioengineered skin substitutes as well as biologics. Commercially available dermal matrix products, such as PROMOGRAN PRISMA™ Matrix made of 44% oxidized regenerated cellulose (ORC), 55% collagen and 1% silver-ORC in a sterile, freeze-dried composite and OASIS® Wound Matrix made of extracellular matrix (collagen, glycosaminoglycans, fibronectin) derived from porcine small intestinal submucosa, have demonstrated significant wound healing advantages over conventional therapy in clinical trials [4–6]. The successful outcomes attributed to the OASIS® Wound Matrix are partially due to the endogenous growth factor content (i.e. basic fibroblast growth factor (bFGF) and transforming growth factor-beta 1 (TGF-β1)) [7]. In some cases, it is advantageous to directly apply growth factors to the wound in order to avoid using biopolymers, which can have poor stability in the chronic wound environment, low mechanical strength and/or illicit an immune response [8]. Several growth factors have been used in wound treatment. In Japan, recombinant human bFGF product (Fiblast® Spray) has been commercially available since 2001 for decubitus ulcers and skin ulcers [9]. Recombinant human epidermal growth factor (EGF) is used in several commercially available products intended for treating diabetic foot ulcers, including Regen-D™ 150 (India), and Easyef® (South Korea). In the United States (US), Regranex® [platelet derived growth factor (PDGF)] is the only drug therapy that has been approved by the Food and Drug Administration (FDA) for the treatment of chronic wounds and it is limited to the treatment of diabetic foot ulcers [10, 11]. Since it entered the market in 1997, no new drug therapies have reached the market in the US. This is unfortunate since clinical studies have shown that only 50% of ulcers treated with Regranex® for 20 weeks healed [12] and the overall performance of topically applied growth factors to treat chronic wounds has been modest [13]. Additionally, increasing severity of the chronic wound further lowers the probability for a successful outcome [14]. The inadequate success rates for topically applied growth factors shows that there is a clear, unmet clinical need for novel drug therapies.

Bioengineered three-dimensional (3D) *in vitro* models have been previously used to aid in the development and toxicity screening of new drug therapies [15–20]. For instance, *in vitro* skin models composed of fibroblasts and keratinocytes in a 3D viscose rayon scaffold were created to test for irritants [21], as well as a 3D multilayered reconstructed human epidermal cellular construct (EpiDerm™) derived from human infant foreskin keratinocytes that closely resembles human epidermis [22]. The *in vitro* skin models developed to measure wound closure have been as simple as monolayer cultures of keratinocytes [23], fibroblasts [24], or both [25], to the more complex single cell three-dimensional cultures [26], and three-dimensional co-cultures [27]. Single cell monolayers remain the most commonly used system due to their simplicity and cost-effectiveness, however, three-dimensional models more accurately represent the complexity of human physiology [28, 29]. For instance, O'Leary et al. fabricated a skin equivalent by seeding keratinocytes onto the upper surface of a collagen scaffold populated with fibroblasts and culturing at the air–liquid interface [30]. Immunostaining of migrating keratinocytes in wounded skin equivalents showed integrin and matrix metalloproteinases expression comparable to normal skin. More recently, a skin equivalent was developed from de-cellularized epidermis that was re-seeded with keratinocytes and fibroblasts and was used to test the effect of two wound healing therapies in wounded skin equivalents [31]. The investigators reported that an untreated wound would heal itself and that both wound healing therapies further promoted healing.

This paper builds upon previous research, which studied the impact of fibrin formulation on both the resulting hydrogels mechanical properties as well as the behavior of fibroblasts and keratinocytes in 3D cell culture [26, 32–38], to fabricate a 3D wound healing model made of a collagen type I construct with fibrin-filled defects. Over 7 days, keratinocyte migration onto the fibrin-filled defects was measured in the presence of fibroblasts and changes in the construct's mechanical properties were monitored. This 3D wound healing model allows for the control over the mechanical and physiological environment cells are exposed to and can be used to investigate cell behavior for each cell type including cell proliferation, migration and differentiation. Furthermore, this 3D construct is a step towards developing a mimetic wound healing model that recapitulates the complex microenvironment of healing wounds. This could aid in the early study of novel therapeutics that promote migration and proliferation of epithelial cells for patients suffering from chronic wounds.

2 Materials and methods

2.1 Cell culture

Human foreskin fibroblasts (HFF; ATCC® SCRC-1041, Manassas, VA, USA) were cultured in Dulbecco's modified Eagle's Medium (DMEM) (Corning, Manassas, VA, USA) with 4.5 mg/mL glucose and supplemented with 10% fetal bovine serum and 1% penicillin/streptomycin.

Human epithelial keratinocytes (HEK; ATCC® CRL-2404, Manassas, VA, USA) were cultured in keratinocyte serum-free media (Life Technologies, Carlsbad, CA, USA). All cells were cultured at 37 °C in 5% carbon dioxide (CO_2) (Shel Lab, model 2375-T, Cornelius, OR, USA). Culture medium was replaced every 2–3 days and the cells were passaged when they were ≥ 80% confluent (approximately every 5–7 days). At the time of experiment, 300,000 HEKs were seeded on top of the construct, and HFFs were seeded either embedded in fibrin beads or dispersed throughout collagen. Constructs containing both keratinocytes and fibroblasts were cultured in keratinocyte serum-free media, which was previously shown to support both fibroblast and keratinocyte proliferation [33]. The constructs were incubated at 37 °C in 5% CO_2 for up to 7 days, and culture medium was replaced every 2–3 days. Keratinocyte migration, cell growth and changes in mechanical stiffness of the scaffold were analyzed at days 1, 3 and 7.

2.2 Scaffold preparation

Control constructs: Collagen constructs were prepared by mixing 200 µL of PureCol bovine collagen (3 mg/mL; Advanced BioMatrix, San Diego, CA, USA) with 25 µL of 10% PBS (Corning Cellgro, Manassas VA, USA) and phenol red (Sigma Aldrich, St. Louis, MO, USA) and 42 µL 0.1 N NaOH (Sigma Aldrich, St. Louis, MO, USA) in the well of a 24-well plate. The final collagen concentration was 2.4 mg/mL. The collagen constructs were allowed to polymerize at 37 °C in 5% CO_2 for 75 min. A second collagen layer was prepared and polymerized in the same manner to create a 3D collagen matrix. Once the second layer of collagen was polymerized, keratinocytes were introduced on top of the construct at a concentration of 300,000 cells/mL. The constructs were placed in the incubator for 3 h to allow the keratinocytes to adhere to the collagen surface. After 3 h, the excess media was aspirated and the surface was washed with PBS. An upside-down 2 µL micropipet tip was inserted into the collagen construct, gently rotated to form the circular outline of a wound and quickly removed—the punching process took less than 5 s to complete. The collagen within this wound was aspirated out and the area was filled in with 30 µL fibrin. Briefly, the fibrinogen component of the Tisseel™ fibrin sealant kit (Baxter Healthcare Corp., BioScience, Westlake Village, CA, USA) was reconstituted with the aprotinin solution following the manufacturer's instructions, and subsequently diluted with 1X tris buffered saline (TBS). Note this component is not a purified source of fibrinogen and may contain trace amounts of growth factors, enzymes as well as extracellular matrix proteins [39]. It was then mixed with the thrombin component of the Tisseel™ fibrin sealant kit, which was reconstituted and diluted with a solution of 40 mM calcium chloride in TBS. This process was repeated twice in each well plate. The fibrin was then allowed to polymerize for 10 min in the incubator. Finished constructs were stored in the incubator with 1 mL keratinocyte serum-free media. Fluorescent images of keratinocytes stained with Vybrant DiD (red) (Invitrogen, Carlsbad, CA, USA) seeded on top of the constructs are shown in Fig. 1 and an illustration of the construct is shown in Fig. 1D.

The first experimental construct introduced fibroblasts directly in the collagen layers (i.e. no fibrin beads). The 3D constructs were prepared in the same manner as the control, but the collagen solution was mixed with fibroblasts after the neutralization of the solution via the addition of PBS and NaOH. The cell concentration was chosen such that an equal number of fibroblasts would be present in both experimental constructs. Keratinocytes were introduced on top of the construct at a concentration of 300,000 cells/mL, and the concentration of the fibrin-filled defect was 10 mg/mL prepared with 10 units/mL thrombin. An illustration of the construct is shown in (Fig. 1E).

The second experimental construct introduced fibroblasts via fibrin beads: The first layer of the collagen scaffold was prepared as above. 10 µL of fibrinogen containing fibroblasts (2000 cells/µL) was pipetted onto each side of the construct, followed by 10 µL of thrombin to form two fibroblast-containing fibrin beads on each construct. The final fibrin concentrations were 5 or 10 mg/mL (F5 or F10) and polymerized with 5 or 10 units/mL of thrombin (T5 or T10). A second layer of collagen was formed above the fibrin beads. Fluorescent images of fibroblasts stained with Vybrant DiO (green) (Invitrogen, Carlsbad, CA, USA) and encapsulated in fibrin beads is shown in Fig. 1B. The remainder of the construct was prepared as previously described above with 300,000 cells/mL of keratinocytes being seeded on top of the construct once the second layer of collagen polymerized, and the concentration of the fibrin-filled defect matched the fibrin bead formulations. A combined fluorescent image of Vybrant DiD-stained keratinocytes seeded on top of the constructs and Vybrant DiO-stained fibroblasts encapsulated in fibrin beads are shown in Fig. 1C and an illustration of the construct is shown in Fig. 1F. The mechanical properties of the resulting fibrin gels is impacted by the fibrin microstructure and this is influenced by various parameters, including the concentrations of fibrinogen, calcium and thrombin. For instance, gels prepared with high thrombin concentrations have a tight network comprised of fine fibers, while gels prepared with low thrombin concentrations have greater porosity and thicker fibers [40–42]. It has been previously shown that changes in matrix morphology can regulate cellular migration, morphology and as well as influence the early stages of wound healing [43–45].

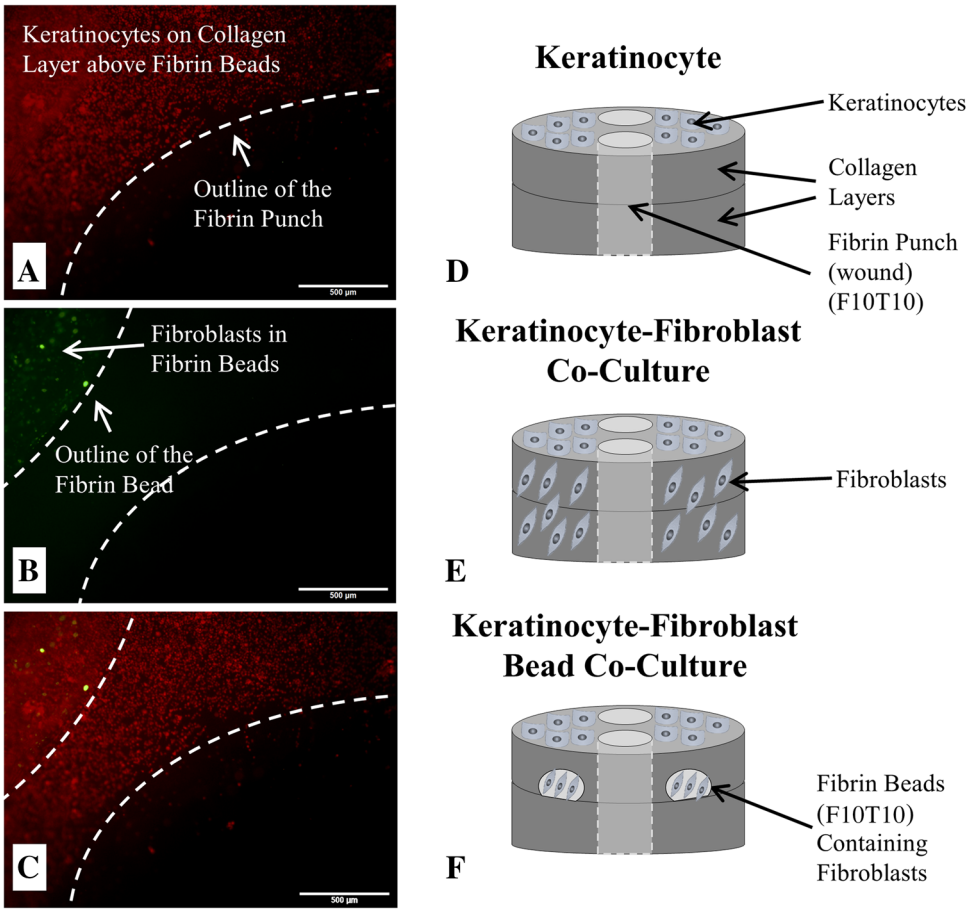

Fig. 1 Micrographs of **A** keratinocytes fluorescently-tagged with Vybrant DiD on the surface of the 3D wound healing construct and near the fibrin-filled defect at a concentration of 300,000 cells/mL; **B** fibroblasts fluorescently-tagged with Vybrant DiO that are encapsulated inside a fibrin bead within the collagen layers of the 3D wound healing construct and near the fibrin-filled defect (20,000 cells/bead); and **C** a stacked fluorescent image of the keratinocyte-fibroblast bead co-culture with fibroblasts encapsulated inside fibrin beads. For all micrographs, the scale bar = 500 µm (50 x magnification). **D** Illustration of the control construct with only keratinocytes seeded on the surface. **E** Illustration of the keratinocyte-fibroblast co-culture construct with fibroblasts uniformly dispersed throughout the collagen matrix and keratinocytes seeded on the surface. **F** Illustration of the keratinocyte-fibroblast bead co-culture with fibroblasts encapsulated inside two fibrin beads within the collagen matrix and keratinocytes seeded on the construct's surface. The final fibrin concentrations were either 5 or 10 mg/mL (F5 or F10) and polymerized with either 5 or 10 units/mL thrombin (T5 or T10). The concentration of the fibrin-filled defect matched the fibrin bead formulation. Note the illustrations are not drawn to scale

2.3 Cell viability and growth assay

Cell viability and growth of fibroblasts and keratinocytes seeded in the wound healing construct (both mono- and co-cultures) was measured using the alamarBlue® assay (Invitrogen, Carlsbad, CA, USA). Fibroblasts were either seeded throughout the collagen construct or within the fibrin beads, and keratinocytes were seeded on top of the collagen construct. The indicator, resazurin, is converted to resorufin—a fluorescent molecule—by the metabolic activity of cells. The fluorescent intensity corresponds to the cells metabolic activity and is proportional to the number of living cells. At each time point (days 1, 3 and 7), the supernatant was aspirated from the 3D constructs and they were washed with warm 1X Dulbecco's phosphate-buffered saline (DPBS) twice prior to the cell growth assay. A 10% solution of alamarBlue® in culture medium was added, and incubated at 37 °C in 5% CO_2 for 4 h. The fluorescence intensity (560 nm excitation, 590 nm emission) of the culture medium was measured using a multi-well plate reader (Inifinite® F200; Tecan Group Ltd., Männedorf, Switzerland).

2.4 Keratinocyte migration

Keratinocyte migration was monitored by collecting images every day starting at day 1 and going through 7, or until the cells reached the center of the fibrin-filled defects, whichever happened first (Fig. 2). Bright field images were captured with an inverted IX71 Olympus microscope

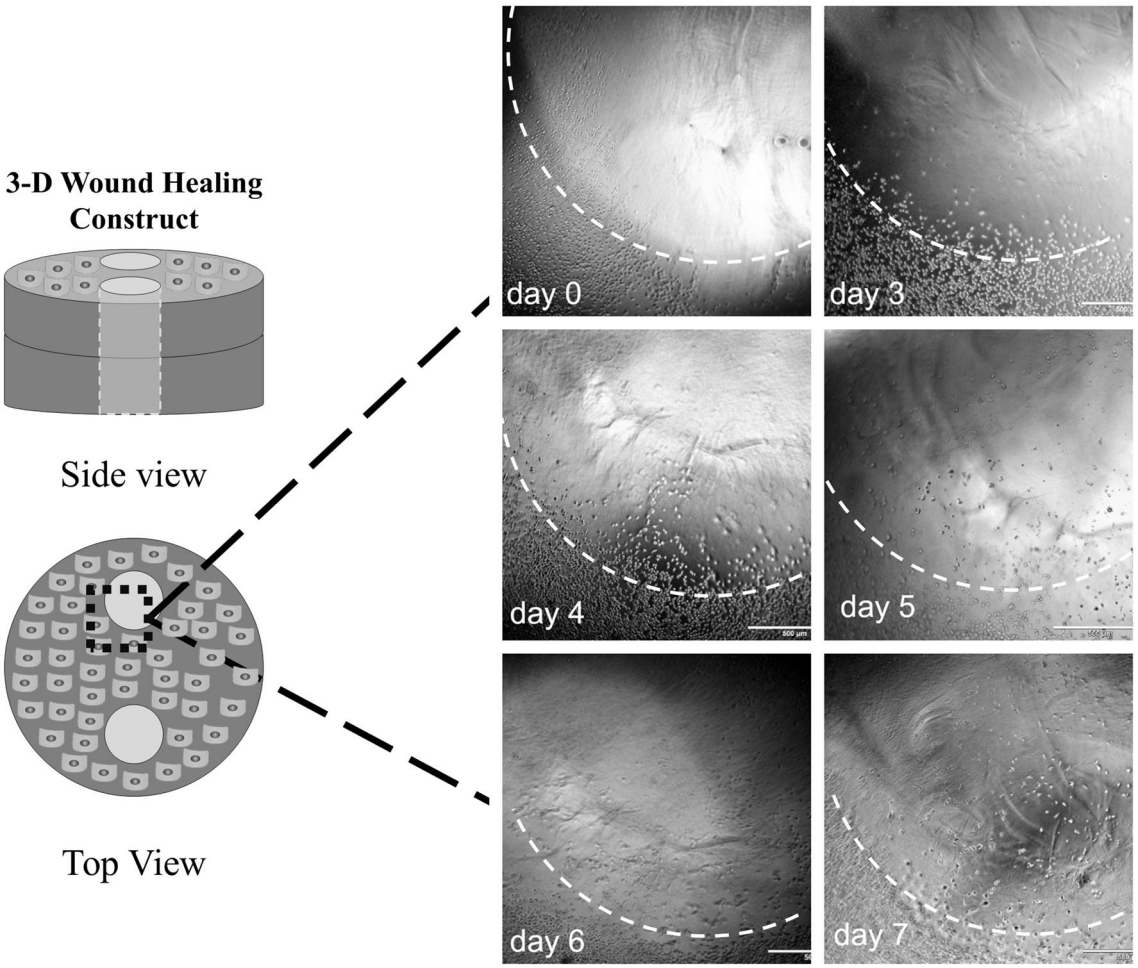

Fig. 2 Representative bright field images used to measure keratinocyte migration toward the center of fibrin-filled defect (wound) in the 3D collagen constructs from day 0 to day 7 (scale bar = 500 μm). The perimeter of the fibrin wound is marked with a dashed white line. Diagram shows the region of interest used to measure keratinocyte migration. Note the illustrations are not drawn to scale

(Olympus America, Center Valley, PA, USA). The images were analyzed using ImageJ software to measure the migration distance from the edge of the fibrin wound toward the center. The migration distance was quantified by averaging the radial migration distance from 10 points around one fibrin wound.

2.5 Mechanical testing of 3D *in vitro* wound healing model

The mechanical stiffness of the 3D wound healing model was monitored using a previously described compressive indentation measurement using an Instron 5564 Universal Testing Machine (Instron, MA, USA) with a 2.5 N load cell. At the time of experiment (days 1, 3 and 7), the excess media was removed from the constructs and they were compressed with a cylindrical flat-ended stainless-steel indenter at a controlled displacement until a final displacement of 2 mm was reached. The Boussinesq elastic solution for a flat punch indentation was used to analyze the linearized portion of the force displacement data (between 0.0 and 1.0 mm) in order to estimate the Young's modulus, E (Eq. 1) [46, 47].

$$F = \left(\frac{2aE}{1-\nu^2}\right)u \tag{1}$$

A Poisson's ratio, υ, of 0.25 was assumed for the constructs [32, 47]. The punch radius, a, was 1.5 mm, and the load force, F, was applied at a rate of 5 mm/min. As previously mentioned, the displacement, u, was 1 mm.

2.6 Statistical analysis

Data are presented as mean ± standard deviation from three or more experiments with each experimental set done in triplicates. A Welches ANOVA and Games-Howell post hoc test were used to compare the mean migration distance of keratinocytes at days 3 and 6 from the six independent

sample groups. A student's t test was performed in comparing means for proliferation over time for each construct as well as changes in the Young's modulus. For all statistical tests performed, $p < 0.05$ was considered statistically significant, and $p < 0.01$ was considered highly significant. The SPSS statistical software package 24.0 for Windows (IBM, Armonk, NY, USA) was used for statistical analysis.

3 Results

This novel wound healing construct provides a tunable microenvironment to study cell behaviors, such as migration, growth, and cross-talk between different cell types. For instance, the mechanical characteristics of both the collagen construct and the fibrin-filled defects can be readily altered by changing the concentrations of collagen and fibrin (i.e. total mass of protein) used in the fabrication of the wound healing model, which alters the biopolymer chain density [40]. This allows the stiffness to be modulated as well as the construct's porosity and the density of binding motifs available to cells present in the construct. While not studied here, it has been previously shown that fibrin and collagen have binding motifs for fibroblasts and keratinocytes. For instance, keratinocytes and fibroblasts both express $\alpha_2\beta_1$, which directly binds on collagen type I, and fibroblasts express $\alpha_v\beta_3$, which binds to fibrinogen at RGD sites [48–50]. Additionally, the use of fibrin beads creates a way to introduce different cell types into the construct in a way that allows for the customization of each cell's microenvironment, which can be optimized to produce cells that match phenotype criterion of native tissue. In this study, keratinocyte behavior in the presence of fibroblasts was examined in three different types of 3D collagen constructs: (1) a control construct where keratinocytes were seeded on the top of the 3D collagen matrix containing fibrin-filled wounds; (2) an experimental construct where fibroblasts are distributed uniformly throughout the collagen matrix; and (3) experimental constructs where fibroblasts are encapsulated in fibrin beads that are embedded in the collagen construct.

3.1 Cell growth greatest in monoculture constructs

Analysis of cell growth by alamarBlue® over a period of 7 days showed that the keratinocytes and fibroblasts were viable and proliferated (Fig. 3). First, keratinocyte and fibroblast cell growth was measured individually—keratinocytes seeded on the top of the constructs and fibroblasts within the constructs—followed by co-cultures. There was an overall increase in cell growth when fibroblasts were cultured alone (Fig. 3A). When fibroblasts were encapsulated in F5T5 beads, there was a statistically significant increase from days 1 to 7. Similarly, there was a statistically significant increase in cell growth from days 1 to 7 when fibroblasts were encapsulated in F5T10 beads. Overall, when the fibrinogen concentration was held constant at 5 mg/mL and thrombin was increased from 5 to 10 units/mL, the total increase in cell growth by day 7 decreased from 1.35 fold increase to 1.20 fold increase, respectively. Increasing the fibrinogen concentration used to fabricate the beads from 5 mg/mL to 10 mg/mL produced significant increases in fibroblast growth. Fibroblasts encapsulated in F10T5 beads had a statistically significant 3.36 fold increase from days 1 to 3, and a slight increase between day 3 and day 7 that was not statistically significant. Likewise, fibroblasts encapsulated in F10T10 beads had a statistically significant 2.31 fold increase in cell growth from days 1 to 3, and no statistically significant change in growth between days 3 and 7. Again, when the fibrinogen concentration was held constant—this time at 10 mg/mL—and the thrombin concentration is increased from 5 to 10 units/mL, the total cell growth on day 7 decreased from 3.39 fold increase to twofold increase, respectively.

A summary of keratinocyte growth in the presence of fibrin-filled wounds prepared with concentrations of fibrinogen and thrombin matching the fibrin beads is shown in Fig. 3B. When exposed to F5T5 fibrin-filled wounds, keratinocytes had a statistically significant 1.39 fold increase in growth between days 1 and 3 but no statistically significant difference between days 3 and 7. A similar trend was observed with F5T10 fibrin-filled wounds. There was a statistically significant 1.43 fold increase in growth between days 1 and 3, and no statistically significant difference between days 3 and 7. When the fibrinogen concentration was held constant at 5 mg/mL, there was a 1.35 fold increase in cell growth by day 7 for both concentrations of thrombin tested. When keratinocytes were in the presence of F10T5 fibrin-filled wounds, there was a 1.13 fold increase in growth between days 1 and 3, and no statistically significant growth between day 3 and 7. The keratinocytes cultured on constructs with F10T10 fibrin-filled wounds had 1.53 fold increase in growth between days 1 and 3, but by day 7 there was an overall 1.38 fold increase in growth compared to day 1. In summary, keratinocyte growth in all the constructs containing fibrin-filled wounds was statistically significant between days 1 and 3.

Constructs containing co-cultures of fibroblasts and keratinocytes experienced little change in growth between days 1, 3, and 7 (Fig. 3C). Specifically, constructs containing F5T5 fibrin-filled wounds and beads had no significant difference in cell growth between days 1 and 7. Similarly, when the fibrin-filled wounds and beads were fabricated using F5T10, there was no statistically

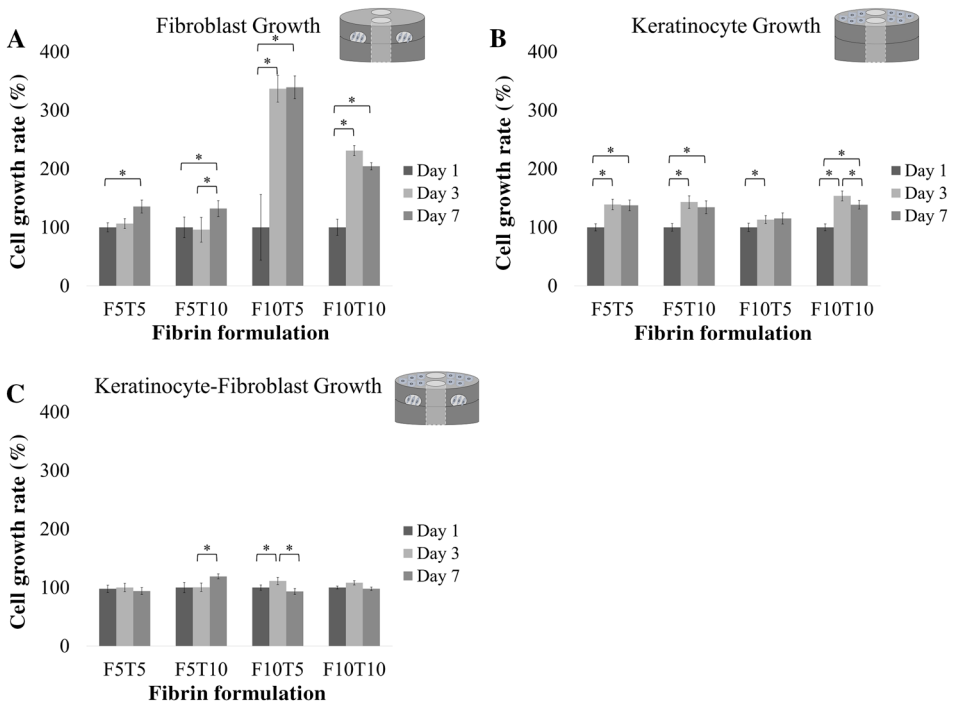

Fig. 3 Comparing the cell growth of **A** fibroblast monocultures, **B** keratinocytes monocultures and **C** fibroblast-keratinocyte co-cultures in 3D wound healing constructs at days 1, 3, and 7 measured by alamarBlue® (n = 9). The x-axis shows the fibrin-bead and wound concentrations in mg/mL (when present; see illustration insert) and the thrombin concentration used for polymerization in units/mL. The collagen concentration was 2.4 mg/mL. Cell growth data is presented as a percentage of day 1 and error bars represent standard deviation. "Asterisks" indicates $p < 0.05$ when comparing cell growth between timepoints

significant difference in proliferation between days 1 and 3. There was a 1.2 fold increase in growth between days 3 and 7. In both the F10T5 and F10T10 constructs, there was no statistically significant difference in growth between days 1 and 7. The overall growth of keratinocytes in the presence of fibroblasts at day 7 was compared to the sum of keratinocyte growth and fibroblast growth that was measured independently (Fig. 4). The fluorescence intensity of the cells in each construct, which was proportional to the number of cells. In nearly all cases, the sum of the fluorescence intensity of keratinocytes and fibroblasts alone was greater than the fluorescence intensity from when both cells were present within the same construct. Specifically, the constructs with F5T5, F5T10 and F10T10 fibrin-filled wounds and beads had statistically significant differences between the co-cultures and the sum, while there was no significant difference for the constructs with F10T5 fibrin-filled wounds and beads.

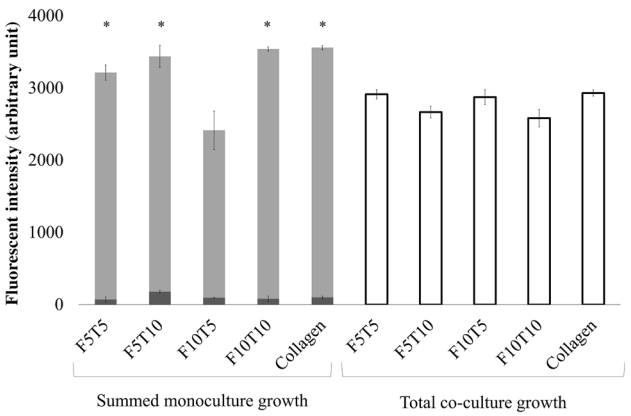

Fig. 4 Comparing the total cell growth of fibroblast-keratinocyte co-cultures with the sum of cell growth from fibroblast and keratinocyte monocultures in 3D wound healing constructs at day 7 measured by alamarBlue® (n = 9). The dark gray bars represent fibroblast growth in monoculture, the light gray bars represent keratinocyte growth in monocultures, and the white bars represent the total cell growth in the co-cultured constructs. The x-axis shows the fibrin-bead and wound concentrations in mg/mL (when present) and the thrombin concentration used for polymerization in units/mL. The collagen concentration was 2.4 mg/mL. "Asterisks" indicates $p < 0.05$ when compared with cell growth in the co-cultured constructs

3.2 Keratinocyte migration increased in the presence of fibroblasts

Keratinocyte migration towards the center of the fibrin wound was analyzed over a period of 7 days (Fig. 5) and demonstrated a step-wise migration behavior when cultured alone. Migration was linear between days 0 and 3 followed by an increase in the migration rate to 278 μm/day between days 3 and 5, and then slowed from days 5 to 7. Migration distance was not recorded past day 7 since the cells had reached the center of the fibrin wound. Keratinocyte migration was accelerated by the presence of fibroblasts within the collagen construct, and the keratinocytes reached the center of the fibrin-defect by day 3 (Fig. 5A). The average migration rate was 388 μm/day. When the fibroblasts were introduced to the collagen construct via fibrin beads, the keratinocyte migration rate decreased compared to keratinocyte-fibroblast co-cultures

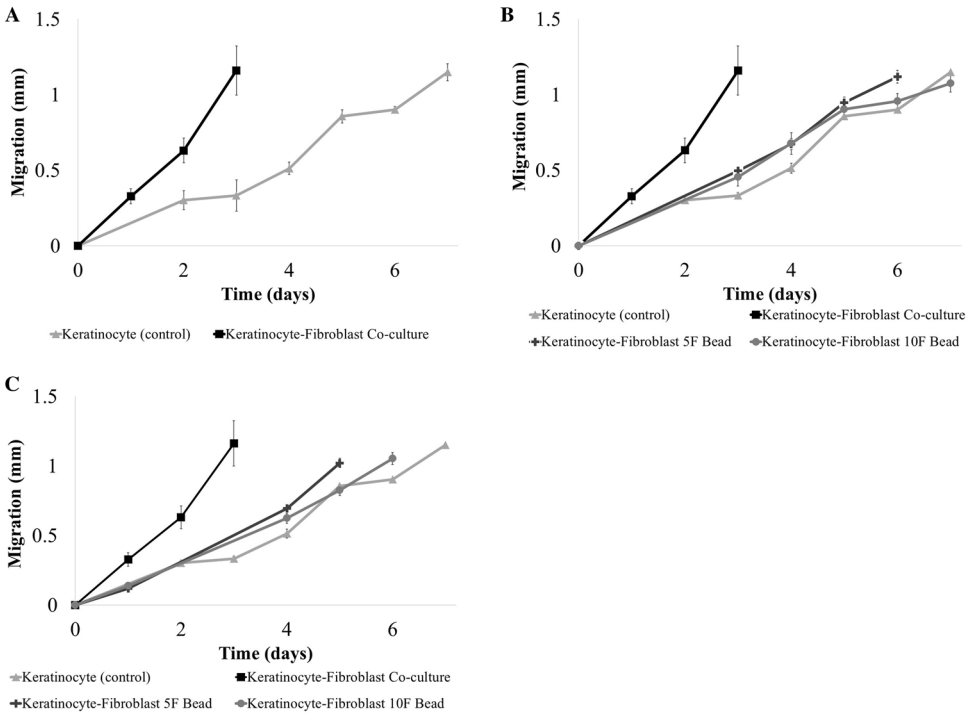

Fig. 5 Comparing the migration of keratinocytes alone (control) and co-cultured with **A** fibroblasts uniformly dispersed throughout the collagen layers, **B** fibroblasts encapsulated in fibrin beads (5 or 10 mg/mL) prepared with 10 units/mL of thrombin, and **C** fibroblasts encapsulated in fibrin beads (5 or 10 mg/mL) prepared with 5 units/mL of thrombin. Overall, the presence of fibroblasts increased the keratinocyte migration rate when compared with keratinocyte monoculture constructs. For all constructs, the collagen concentration was 2.4 mg/mL and the fibrin wound composition matched the fibrin bead composition ($n \geq 9$). The error bars represent standard deviation

without fibrin beads. However, the migration rate was higher than keratinocyte-only constructs. Specifically, the average migration rate was 153 μm/day when the fibroblasts were encapsulated in fibrin beads prepared with 10 mg/mL fibrinogen and 10 units/mL thrombin (F10T10), and 172 μm/day when the fibroblasts where encapsulated in F5T10 beads (Fig. 5B). Lowering the concentration of thrombin used to prepare the fibrin beads encapsulating the fibroblasts increased the average keratinocyte migration rate: 176 μm/day in constructs with F10T5 beads and 202 μm/day in constructs with F5T5 beads (Fig. 5C).

Statistical analysis using Welches ANOVA and Games-Howell post hoc test to compare the migration distance between the independent groups at days 3 and 6 showed that there was a statistically significant difference ($p < 0.05$) among the migration distance of all the groups at day 3. Additionally, there was a highly significant ($p < 0.01$) differences among all the groups except the constructs containing fibrin beads prepared with 5 units/mL thrombin. By day 6, the keratinocyte-fibroblast co-culture construct and the construct with the 5F5T beads had reached the center of the fibrin wound—day 3 and day 5, respectively. The remaining groups showed highly significant ($p < 0.01$) differences except between the F10T10 bead and the keratinocyte-only constructs, which had no statistically significant difference in migration distance at day 6. Migration results are summarized in Table 1.

3.3 Mechanical stiffness constant in co-culture constructs

Instron compression testing was done to analyze the change in stiffness of collagen constructs over 7 days. Stiffness is a measure of a material's resistance to deformation and is calculated as the slope of the stress versus strain plot—also known as the Young's modulus [51]. The absolute modulus of the 3D constructs on Day 1 is shown in the Supporting Information Fig. 1. For the constructs seeded with fibroblasts only, there was no statistically significant change in the stiffness except for a statistically significant decrease in stiffness between days 1 and 7 for constructs containing F5T5 and F5T10 fibrin-filled wounds and beads (Fig. 6A). When keratinocytes were seeded alone in the constructs, there was an increasing trend in stiffness from day 1 to 7 (Fig. 6B). It was statistically significant for all constructs except the F10T10 constructs, which had no statistically significant difference between days 1 and 7. When both cell types were introduced to the construct, there was no statistically significant changes in stiffness (Fig. 6C).

4 Discussion

The goal of this study was to fabricate a 3D wound healing model comprised of a collagen type I scaffold with fibrin-filled defects in order to assess keratinocyte migration for

Table 1 Summary of keratinocyte migration

Construct	Center by day	Avg. migration rate (μm/day)
Keratinocyte (control)	7	153
F10T10 beads	7	164
F5T10 beads	6	186
F10T5 beads	6	176
F5T5 beads	5	204
Keratinocyte-fibroblast co-culture	3	387

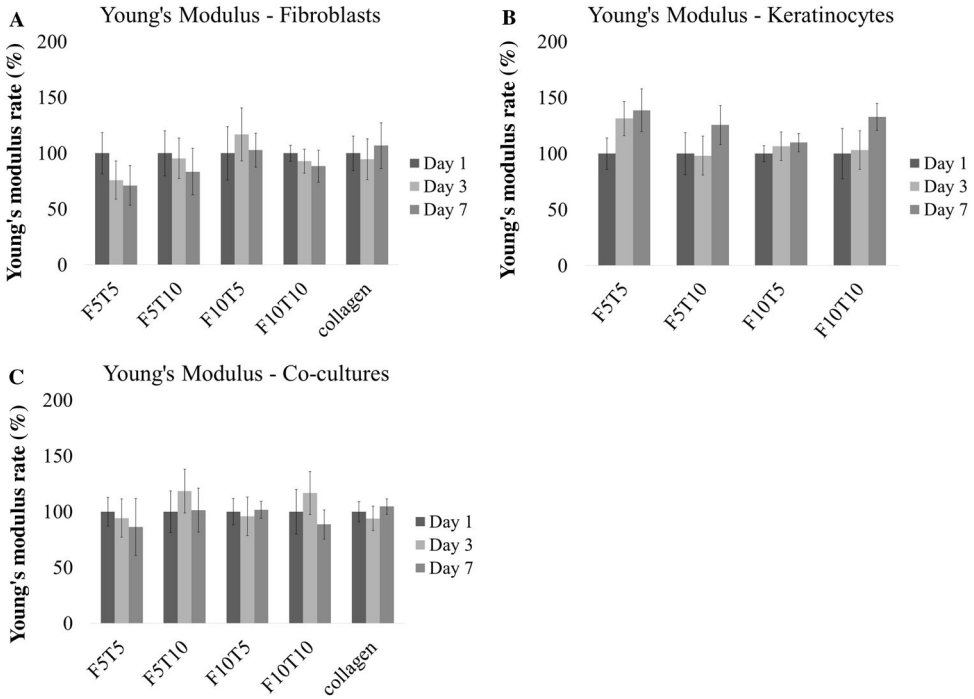

Fig. 6 The change in Young's Modulus, E, of 3D wound healing constructs seeded with **A** fibroblasts only, **B** keratinocytes only, and **C** fibroblast-keratinocyte co-cultures at days 1, 3, and 7 measured as measured by compressive indentation testing ($n \geq 9$). Data is presented as a percentage of day 1 and error bars represent standard deviation

up to 7 days in the presence and absence of fibroblasts. Fibrin beads were introduced into the 3D construct in order to control the spatial arrangement of fibroblasts relative to keratinocytes as well as to control the fibroblast's microenvironment. In addition to measuring changes in keratinocyte migration, cell growth and changes in mechanical properties of the construct were also investigated. This study demonstrated that the 3D construct can be used to control inputs, such as varying local cell-seeding density independent of cell number, spatial arrangement between cells and extracellular matrix composition, and measure cellular response. Additionally, the results are a step towards developing a mimetic wound healing model that recapitulates the complex wound healing microenvironment, but it is currently incomplete. *In vivo*, the wound healing process involves many cell types not investigated in this study, including platelets, endothelial cells, macrophages, neutrophils, and myofibroblasts as well as the numerous growth factors, cytokines and chemokines that they secrete [1]. The complexity of the wound healing model developed in this study can be increased simply with the addition of signaling molecules and other cell types to features of the construct, such as the fibrin-filled defect and fibrin beads. Understanding the effects paracrine signaling between multiple cell types and their relative spatial arrangements have on the cellular components will be important for the future development of therapies for patients suffering from chronic wounds.

Keratinocyte migration results demonstrated that the presence of fibroblasts within the construct increased migration when compared against constructs seeded with keratinocytes only. Similar results have been reported in a previous study investigating keratinocyte migration when co-cultured with fibroblasts. Specifically, significant keratinocyte migration was observed when the two cell types were in direct contact with each, but there was no change in keratinocyte migration compared to keratinocyte-only controls when a transwell was used to separate the two cell types [25]. In this study, keratinocyte migration was fastest when fibroblasts were dispersed throughout the 3D

collagen construct, which allowed direct contact with keratinocytes seeded on top of the collagen. Sequestering the fibroblasts within fibrin beads embedded within the collagen construct decreased keratinocyte migration; however, migration was still greater than when there was no fibroblasts present. Additionally, decreasing the fibrin concentration of the fibrin beads promoted faster keratinocyte migration. This lab has previously shown that fibrinogen and thrombin concentration are inversely related to fibrin gel porosity, pore size, and permeability [35]. Consequently, there is less impendence to paracrine signaling between encapsulated fibroblasts and keratinocytes. In previous studies, expression levels of both TGF-β and b-FGF—measured by ELISA—significantly increased in fibroblasts co-cultured with keratinocytes for 3 days when compared with control fibroblasts or keratinocytes in mono culture [52]. It has been previously shown that both these growth factors have an influence on keratinocyte migration. Specifically, bFGF stimulated keratinocyte migration when cultured on type I collagen-coated substrates [53], and TGF-β was shown to induce keratinocytes to express integrins that facilitate migration [54]. Interestingly, keratinocytes lack the expression of integrin $\alpha_v\beta_3$—the receptor for fibrin [55]. However, keratinocytes can express four fibronectin-binding integrins: $\alpha_5\beta_1$, $\alpha_3\beta_1$, $\alpha_8\beta_1$, $\alpha_v\beta_6$ [56], and the fibrin used for this study has been previously reported to contain 6 mg/mL of fibronectin (undiluted) [38, 39]. However, more research using a purified fibrin source is needed to elucidate the role plasma proteins within fibrin sealant have on cell migration.

Changes in migration rate corresponded with changes in cell growth. In the fibroblast and keratinocyte co-cultures, there was little-to-no growth measured over the 7 days, but there was an increase in keratinocyte migration. In addition to promoting keratinocyte migration as previously discussed, TFG-β has also been shown to inhibit keratinocyte growth. A study of mouse keratinocytes found that the c-myc gene expression was necessary for epithelial cell proliferation and that TFG-β reduced c-myc expression by blocking transcription [57]. This suggests that keratinocyte migration was due to increased cell mobility and not cell growth. There have been previous studies investigating keratinocyte migration that used mitomycin C treatment to arrest cell growth so wound closure results would not be confounded by cell growth [58, 59]. However, they also report that the absence of mitomycin C treatment produced minimal changes in wound closure suggesting the amount of wound closure due to proliferation was minor. The absence of cell growth in the co-cultured constructs differs from a previous study from one of the co-authors, which found that there was a synergistic enhancement of cell growth in fibroblasts and keratinocyte co-cultures. Specifically, the cell proliferation for both keratinocytes and fibroblasts—measured by Magnetic Activated Cell Separation (MACS)—co-cultured in 3D fibrin constructs was greater than the proliferation for either cell type in monocultures [33]. However, differences in the experimental design likely account for the conflicting results. For instance, the previous study incorporated both cell types freely within a 3D fibrin scaffold that were absent of defects filled with extracellular matrix protein that were devoid of cells. In this study, the cells were spatially arranged such that keratinocytes were seeded on top of the collagen scaffold while fibroblasts were embedded within the scaffold, and the cell-free fibrin-filled defects allowed cell migration.

It has been previously documented that the mechanical properties of a hydrogel matrix influences cell behavior, and that cell remodeling can affect a hydrogel's mechanical properties [60–63]. When monocultures of fibroblasts were grown in the collagen constructs, there was a decreasing trend in construct stiffness over time. Migrating fibroblasts leaving the embedded fibrin beads use enzymes such as collagenase and matrix metalloproteases to facilitate migration through a 3D environment [64]. When monocultures of keratinocytes were grown on the surface of collagen constructs, there was a slight increase in construct stiffness, and visible changes to the construct dimension were observed. Specifically, contraction of the collagen constructs caused slight pulling-away of the contrast from the wall of the well plate. High cell seeding densities have been shown to increase hydrogel stiffness due to hydrogel compaction from forces exerted on the matrix by the cells [32]. However, when both fibroblasts in fibrin beads and keratinocytes were incorporated in the collagen constructs, there was no significant change in mechanical modulus overtime. It is likely the opposing effects of fibroblasts and keratinocytes on matrix stiffness could explain these results. It is also beneficial that the mechanical integrity of the construct remains intact since it suggests that it can serve as a viable *in vitro* wound healing model for at least a week.

To model the function of keratinocytes and fibroblasts, commercially available HEK001 and HFF-1 cell lines were utilized in this study. However, previous studies have shown that differences in can exist between primary cells and cell lines as well as between different cell lines [65, 66]. For instance, a study of Toll-like receptor (TLR) expression on different keratinocyte cell lines as well as primary keratinocytes and their chemokine production in response to TLR-ligand binding showed that differences exists between the different cell lines [65]. Specifically, HEK001 cells overexpressed TLR2 and TLR5. TLR2 is used by keratinocytes to detect peptidoglycan and lipoteichoic acid, and expression of TLR5 is characteristic of basal layer keratinocytes. In this instance, cell choice

would significantly impact a study of the innate immune response using the reported wound healing model, and it likely that differences also exist in levels of integrin and cytokine expression between the different cell lines, which have not yet been fully investigated. Therefore, future studies using both primary fibroblasts and keratinocytes as well as different cell lines would verify the efficacy of this construct to serve as an *in vitro* wound healing model.

In summary, this data shows that keratinocyte migration is enhanced by the presence of fibroblasts in wound healing models made of collagen type I with fibrin-filled defects. The greatest keratinocyte migration was observed in constructs where fibroblasts were seeded throughout the collagen construct and not in the fibrin beads. It was also observed that the constructs with the greatest keratinocyte migration rates were also the constructs with the least cell growth suggesting fibroblasts promote keratinocyte migration over proliferation in "wounded" constructs. Furthermore, the cellular response was influenced by the presence of fibrin beads and could be modulated by changes to the fibrin concentration within the beads as demonstrated by the changes in keratinocyte migration when fibroblasts were encapsulated in fibrin beads. This simplified wound healing model is an early step towards recapitulating the complex microenvironment of healing wounds *in vitro*, and fibrin beads can be used to create custom microenvironments for other cell types involved in wound healing, such immune and vascular cells. Furthermore, the fibrin beads in this study can be used in future studies to control the presentation of signaling molecules as well as different cell types present in the wound-healing *milieu*. In general, this approach is useful for engineering the cellular microenvironment such that the interactions between cell types can be controlled in order to better study topics in developmental biology as well as to optimize efficacious tissue engineered products.

Acknowledgements The authors acknowledge funding support from the National Institute of Arthritis and Musculoskeletal and Skin Diseases of the National Institutes of Health under Award Number R21AR064437. The content is solely the responsibility of the authors and does not necessarily represent the official views of the funding sponsors.

Compliance with ethical standards

Conflicts of interest The authors have no financial conflicts of interest.

Ethical approval There are no animal experiments carried out for this article.

References

1. Eming SA, Martin P, Tomic-Canic M. Wound repair and regeneration: mechanisms, signaling, and translation. Sci Transl Med. 2014;6:265sr6.
2. Sen CK, Gordillo GM, Roy S, Kirsner R, Lambert L, Hunt TK, et al. Human skin wounds: a major and snowballing threat to public health and the economy. Wound Repair Regen. 2009;17:763–71.
3. Snyder RJ, Kirsner RS, Warriner RA 3rd, Lavery LA, Hanft JR, Sheehan P. Consensus recommendations on advancing the standard of care for treating neuropathic foot ulcers in patients with diabetes. Ostomy Wound Manage. 2010;56:S1–24.
4. Romanelli M, Dini V, Bertone MS. Randomized comparison of OASIS Wound Matrix versus moist wound dressing in the treatment of difficult-to-heal wounds of mixed arterial/venous etiology. Adv Skin Wound Care. 2010;23:34–8.
5. Mostow EN, Haraway GD, Dalsing M, Hodde JP, King D; OASIS Venus Ulcer Study Group. Effectiveness of an extracellular matrix graft (OASIS Wound Matrix) in the treatment of chronic leg ulcers: a randomized clinical trial. J Vasc Surg. 2005;41:837–43.
6. Gottrup F, Cullen BM, Karlsmark T, Bischoff-Mikkelsen M, Nisbet L, Gibson MC. Randomized controlled trial on collagen/oxidized regenerated cellulose/silver treatment. Wound Repair Regen. 2013;21:216–25.
7. Hu MS, Maan ZN, Wu JC, Rennert RC, Hong WX, Lai TS, et al. Tissue engineering and regenerative repair in wound healing. Ann Biomed Eng. 2014;42:1494–507.
8. Badylak SE, Gilbert TW. Immune response to biologic scaffold materials. Semin Immunol. 2008;20:109–16.
9. Okabe K, Hayashi R, Aramaki-Hattori N, Sakamoto Y, Kishi K. Wound treatment using growth factors. Mod Plast Surg. 2013;3:108–12.
10. Papanas N, Maltezos E. Becaplermin gel in the treatment of diabetic neuropathic foot ulcers. Clin Interv Aging. 2008;3:233–40.
11. Long DW, Johnson NR, Jeffries EM, Hara H, Wang Y. Controlled delivery of platelet-derived proteins enhances porcine wound healing. J Control Release. 2017;253:73–81.
12. Hingorani A, LaMuraglia GM, Henke P, Meissner MH, Loretz L, Zinszer KM, et al. The management of diabetic foot: a clinical practice guideline by the Society for Vascular Surgery in collaboration with the American Podiatric Medical Association and the Society for Vascular Medicine. J Vasc Surg. 2016;63:3S–21S.
13. Robson MC, Steed DL, Franz MG. Wound healing: biologic features and approaches to maximize healing trajectories—in brief. Curr Probl Surg. 2001;38:72–140.
14. Berlanga-Acosta J, Fernández-Montequín J, Valdés-Pérez C, Savigne-Gutiérrez W, Mendoza-Marí Y, García-Ojalvo A, et al. Diabetic foot ulcers and epidermal growth factor: revisiting the local delivery route for a successful outcome. Biomed Res Int 2017;2017:2923759.
15. DesRochers TM, Suter L, Roth A, Kaplan DL. Bioengineered 3D human kidney tissue, a platform for the determination of nephrotoxicity. PLoS One. 2013;8:e59219.
16. Chang R, Emami K, Wu H, Sun W. Biofabrication of a three-dimensional liver micro-organ as an in vitro drug metabolism model. Biofabrication. 2010;2:045004.
17. Sung JH, Shuler ML. A micro cell culture analog (mu CCA) with 3-D hydrogel culture of multiple cell lines to assess metabolism-dependent cytotoxicity of anti-cancer drugs. Lab Chip. 2009;9:1385–94.

18. Lan SF, Starly B. Alginate based 3D hydrogels as an in vitro co-culture model platform for the toxicity screening of new chemical entities. Toxicol Appl Pharmacol. 2011;256:62–72.
19. Kirsch-Volders M, Decordier I, Elhajouji A, Plas G, Aardema MJ, Fenech M. In vitro genotoxicity testing using the micronucleus assay in cell lines, human lymphocytes and 3D human skin models. Mutagenesis. 2011;26:177–84.
20. Nakamura K, Mizutani R, Sanbe A, Enosawa S, Kasahara M, Nakagawa A, et al. Evaluation of drug toxicity with hepatocytes cultured in a micro-space cell culture system. J Biosci Bioeng. 2011;111:78–84.
21. Cantòn I, Cole DM, Kemp EH, Watson PF, Chunthapong J, Ryan AJ, et al. Development of a 3D human in vitro skin co-culture model for detecting irritants in real-time. Biotechnol Bioeng. 2010;106:794–803.
22. Hu T, Khambatta ZS, Hayden PJ, Bolmarcich J, Binder RL, Robinson MK, et al. Xenobiotic metabolism gene expression in the EpiDerm^{TM} in vitro 3D human epidermis model compared to human skin. Toxicol Vitro. 2010;24:1450–63.
23. Tao H, Berno AJ, Cox DR, Frazer KA. In vitro human keratinocyte migration rates are associated with SNPs in the KRT1 interval. PLoS One. 2007;2:e697.
24. Bindschadler M, McGrath JL. Sheet migration by wounded monolayers as an emergent property of single-cell dynamics. J Cell Sci. 2007;120:876–84.
25. Wang ZX, Wang Y, Farhangfar F, Zimmer M, Zhang Y. Enhanced keratinocyte proliferation and migration in co-culture with fibroblasts. PLoS One. 2012;7:e40951.
26. Chen ZJ, Yang JP, Wu BM, Tawil B. A novel three-dimensional wound healing model. J Dev Biol. 2014;2:198–209.
27. Gottrup F, Agren MS, Karlsmark T. Models for use in wound healing research: a survey focusing on in vitro and in vivo adult soft tissue. Wound Repair Regen. 2000;8:83–96.
28. Groeber F, Holeiter M, Hampel M, Hinderer S, Schenke-Layland K. Skin tissue engineering—in vivo and in vitro applications. Adv Drug Deliv Rev. 2011;63:352–66.
29. Liang CC, Park AY, Guan JL. In vitro scratch assay: a convenient and inexpensive method for analysis of cell migration in vitro. Nat Protoc. 2007;2:329–33.
30. O'Leary R, Arrowsmith M, Wood EJ. Characterization of the living skin equivalent as a model of cutaneous re-epithelialization. Cell Biochem Funct. 2002;20:129–41.
31. Xie Y, Rizzi SC, Dawson R, Lynam E, Richards S, Leavesley DI, et al. Development of a three-dimensional human skin equivalent wound model for investigating novel wound healing therapies. Tissue Eng Part C Methods. 2010;16:1111–23.
32. Duong H, Wu B, Tawil B. Modulation of 3D fibrin matrix stiffness by intrinsic fibrinogen-thrombin compositions and by extrinsic cellular activity. Tissue Eng Part A. 2009;15:1865–76.
33. Sese N, Cole M, Tawil B. Proliferation of human keratinocytes and cocultured human keratinocytes and fibroblasts in three-dimensional fibrin constructs. Tissue Eng Part A. 2011;17:429–37.
34. Ho W, Tawil B, Dunn JC, Wu BM. The behavior of human mesenchymal stem cells in 3D fibrin clots: dependence on fibrinogen concentration and clot structure. Tissue Eng. 2006;12:1587–95.
35. Chiu CL, Hecht V, Duong H, Wu B, Tawil B. Permeability of three-dimensional fibrin constructs corresponds to fibrinogen and thrombin concentrations. Biores Open Access. 2012;1:34–40.
36. Cole M, Cox S, Inman E, Chan C, Mana M, Helgerson S, et al. Fibrin as a delivery vehicle for active macrophage activator lipoprotein-2 peptide: in vitro studies. Wound Repair Regen. 2007;15:521–9.
37. Cox S, Cole M, Tawil B. Behavior of human dermal fibroblasts in three-dimensional fibrin clots: dependence on fibrinogen and thrombin concentration. Tissue Eng. 2004;10:942–54.
38. Reinertsen E, Skinner M, Wu B, Tawil B. Concentration of fibrin and presence of plasminogen affect proliferation, fibrinolytic activity, and morphology of human fibroblasts and keratinocytes in 3D fibrin constructs. Tissue Eng Part A. 2014;20:2860–9.
39. Buchta C, Hedrich HC, Macher M, Höcker P, Redl H. Biochemical characterization of autologous fibrin sealants produced by CryoSeal and Vivostat in comparison to the homologous fibrin sealant product Tissucol/Tisseel. Biomaterials. 2005;26:6233–41.
40. Rowe SL, Lee S, Stegemann JP. Influence of thrombin concentration on the mechanical and morphological properties of cell-seeded fibrin hydrogels. Acta Biomater. 2007;3:59–67.
41. Blombäck B, Carlsson K, Hessel B, Liljeborg A, Procyk R, Aslund N. Native fibrin gel networks observed by 3D microscopy, permeation and turbidity. Biochim Biophys Acta. 1989;997:96–110.
42. Kubota K, Kogure H, Masuda Y, Toyama Y, Kita R, Takahashi A, et al. Gelation dynamics and gel structure of fibrinogen. Colloids Surf B Biointerfaces. 2004;38:103–9.
43. Dikovsky D, Bianco-Peled H, Seliktar D. The effect of structural alterations of PEG-fibrinogen hydrogel scaffolds on 3-D cellular morphology and cellular migration. Biomaterials. 2006;27:1496–506.
44. Pizzo AM, Kokini K, Vaughn LC, Waisner BZ, Voytik-Harbin SL. Extracellular matrix (ECM) microstructural composition regulates local cell-ECM biomechanics and fundamental fibroblast behavior: a multidimensional perspective. J Appl Physiol (1985). 2005;98:1909–21.
45. Karp JM, Sarraf F, Shoichet MS, Davies JE. Fibrin-filled scaffolds for bone-tissue engineering: an in vivo study. J Biomed Mater Res A. 2004;71:162–71.
46. Mooney RG, Costales CA, Curtin JM, Tawil B, Shaw MC. Indentation micromechanics of fibroblast-populated fibrin constructs. Mater Res Soc Symp Proc. 2005;874:L7.10.
47. Mooney RG, Costales CA, Freeman EG, Curtin JM, Corrin AA, Lee JT, et al. Indentation micromechanics of three-dimensional fibrin/collagen biomaterial scaffolds. J Mater Res. 2006;21:2023–34.
48. Knight CG, Morton LF, Peachey AR, Tuckwell DS, Farndale RW, Barnes MJ. The collagen-binding A-domains of integrins alpha(1)beta(1) and alpha(2)beta(1) recognize the same specific amino acid sequence, GFOGER, in native (triple-helical) collagens. J Biol Chem. 2000;275:35–40.
49. Gailit J, Clarke C, Newman D, Tonnesen MG, Mosesson MW, Clark RA. Human fibroblasts bind directly to fibrinogen at RGD sites through integrin alpha(v)beta3. Exp Cell Res. 1997;232:118–26.
50. Scharffetter-Kochanek K, Klein CE, Heinen G, Mauch C, Schaefer T, Adelmann-Grill BC, et al. Migration of a human keratinocyte cell-line (HaCaT) to interstitial collagen type-I is mediated by the alpha-2-beta-1-integrin receptor. J Invest Dermatol. 1992;98:3–11.
51. Wells RG. The role of matrix stiffness in regulating cell behavior. Hepatology. 2008;47:1394–400.
52. Nayak S, Dey S, Kundu SC. Skin equivalent tissue-engineered construct: co-cultured fibroblasts/keratinocytes on 3D Matrices of sericin hope cocoons. PLoS One. 2013;8:e74779.
53. Sogabe Y, Abe M, Yokoyama Y, Ishikawa O. Basic fibroblast growth factor stimulates human keratinocyte motility by Rac activation. Wound Repair Regen. 2006;14:457–62.
54. Gailit J, Welch MP, Clark RA. TGF-beta-1 stimulates expression of keratinocyte integrins during reepithilialization of cutaneous wounds. J Invest Dermatol. 1994;103:221–7.
55. Kubo M, Van De Water L, Plantefaber LC, Mosesson MW, Simon M, Tonnesen MG, et al. Fibrinogen and fibrin are anti-adhesive for keratinocytes: a mechanism for fibrin eschar slough during wound repair. J Invest Dermatol. 2001;117:1369–81.

56. Larjava H, Haapasalmi K, Salo T, Wiebe C, Uitto VJ. Keratinocyte integrins in wound healing and chronic inflammation of the human periodontium. Oral Dis. 1996;2:77–86.
57. Pietenpol JA, Holt JT, Stein RW, Moses HL. Transforming growth factor beta 1 suppression of c-myc gene transcription: role in inhibition of keratinocyte proliferation. Proc Natl Acad Sci U S A. 1990;87:3758–62.
58. Draper BK, Komurasaki T, Davidson MK, Nanney LB. Epiregulin is more potent than EGF or TGF alpha in promoting in vitro wound closure due to enhanced ERK/MAPK activation. J Cell Biochem. 2003;89:1126–37.
59. Satish L, Yager D, Wells A. Glu-Leu-Arg-negative CXC chemokine interferon gamma inducible protein-9 as a mediator of epidermal-dermal communication during wound repair. J Invest Dermatol. 2003;120:1110–7.
60. Grinnell F. Fibroblast-collagen-matrix contraction: growth-factor signalling and mechanical loading. Trends Cell Biol. 2000;10:362–5.
61. Stevens MM, George JH. Exploring and engineering the cell surface interface. Science. 2005;310:1135–8.
62. Huang D, Chang TR, Aggarwal A, Lee RC, Ehrlich HP. Mechanisms and dynamics of mechanical strengthening in ligament-equivalent fibroblast-populated collagen matrices. Ann Biomed Eng. 1993;21:289–305.
63. Markowski MC, Brown AC, Barker TH. Directing epithelial to mesenchymal transition through engineered microenvironments displaying orthogonal adhesive and mechanical cues. J Biomed Mater Res A. 2012;100:2119–27.
64. Ghersi G, Dong H, Goldstein LA, Yeh Y, Hakkinen L, Larjava HS, et al. Regulation of fibroblast migration on collagenous matrix by a cell surface peptidase complex. J Biol Chem. 2002;277:29231–41.
65. Olaru F, Jensen LE. Chemokine expression by human keratinocyte cell lines after activation of Toll-like receptors. Exp Dermatol. 2010;19:e314–6.
66. Maas-Szabowski N, Stärker A, Fusenig NE. Epidermal tissue regeneration and stromal interaction in HaCaT cells is initiated by TGF-alpha. J Cell Sci. 2003;116:2937–48.